J Mater Sci (2007) 42:8795–8803
DOI 10.1007/s10853-007-1914-1

Mechanics of molecular collagen is influenced by hydroxyapatite in natural bone

Rahul Bhowmik · Kalpana S. Katti · Dinesh R. Katti

Received: 17 January 2007 / Accepted: 4 June 2007 / Published online: 10 July 2007

Abstract As often seen in biological structural materials, bone exhibits complex hierarchical structure. The primary constituents of bone are collagen and hydroxyapatite (HAP). HAP mineralizes at specific locations at collagen, in such a way that the *c*-axis of HAP aligns parallel to collagen molecule. The collagen molecule is helical overall with non-helical ends that are N- or C-telopeptides. The collagen molecule with telopeptides interacts with specific surfaces of mineralized HAP. When subjected to load, the interactions at the interface between HAP and collagen may significantly affect the overall mechanics of the collagen molecule. Here, we have performed molecular dynamics (MD) and steered MD (SMD) simulations in order to understand the load carrying behavior of collagen in the proximity of HAP. Our simulations indicate that the load-deformation response of collagen is different when it interacts with HAP as compared to its response in the absence of HAP. The interface between HAP and collagen affects the overall load-deformation response of collagen. Further, bone also has considerable amount of water and we have observed that water significantly influences the load-deformation response of collagen due to collagen-water-HAP interactions.

R. Bhowmik · K. S. Katti (✉) · D. R. Katti
Department of Civil Engineering, North Dakota State University, Fargo, ND 58105, USA
e-mail: Kalpana.Katti@ndsu.edu

R. Bhowmik
e-mail: Rahul.Bhowmik@ndsu.edu

D. R. Katti
e-mail: Dinesh.Katti@ndsu.edu

Introduction

Bone is an important structural component of the human body and is a part of the skeletal system. It performs various mechanical, biological, and chemical functions which include: supporting the body structure, protecting internal organs, producing red and white blood cells, and storing various ions [1, 2]. It has a unique capability of self-regeneration under appropriate conditions [3]. Bone exhibits a distinct set of mechanical properties depending on its location in the skeletal system [4]. This is due to the fact that the different p'arts (bone) of the skeletal system undergo different loading paths during normal daily activities [5, 6]. These unique sets of mechanical properties are a result of structural hierarchy in bone [7–9] which encompasses molecular to macroscopic level spanning over several orders of magnitude of length scale as shown in Fig. 1. However, the role of mechanics of various structures at different length scales on overall mechanical response is not clearly understood. This understanding is vital for designing novel implant materials with mechanical properties similar to natural bone [10–14]. Several attempts have been made to understand the mechanical properties of bone and its relation to the hierarchal structural organization [15–31]. Ji et al. have used finite element modeling (FEM) methods to calculate the fundamental mechanical properties of bone [21]. Buehler et al have explained the reasons for the specific length of collagen molecules which is observed in the nanostructure of bone and its mechanical properties by multiscale modeling techniques [22, 23]. Hellmich et al. have examined the mechanical behavior of bone through micromechanics formulations [24, 25]. It has been observed that the young's modulus of cortical bone is in the range of 14–20 GPa [26], whereas that of the osteon lamellar structure is about 22 GPa [27]. However, the

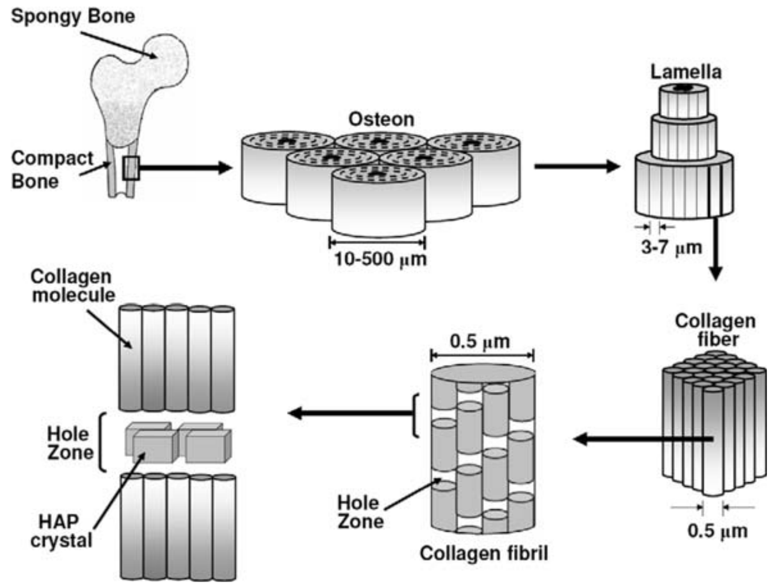

Fig. 1 Schematic showing structural hierarchy in Bone

mechanical response of collagen when mineral has mineralized at specific locations is not known. This is very difficult to obtain from experimental techniques due to small size of mineralized hydroxyapatite crystals (50 nm × 25 nm × 3 nm) and collagen molecule (300 nm) [28–31]. In this present study we have obtained the mechanical response of collagen molecule in proximity of mineral using steered molecular dynamics (SMD) simulations. In our prior work on a biological hybrid system nacre, [32], we have observed marked influence of proximity of mineral on the mechanics of the protein molecule at organic-inorganic interfaces.

Also, it has been observed from experiments that water affects the overall mechanical response of bone. Bone has about 10 % of water in body environment (Table 1) [28, 33–35] and with loss of water, bone exhibits different mechanical properties [36–43]. It has been observed that strain-at-fracture and energy-to-fracture decreases, whereas tensile strength, stiffness, and hardness increases with loss of water [36–41]. Nyman et al. have shown that toughness of bone decreases when water is removed from collagen, whereas both the strength and toughness decrease when water is lost from mineral phase [42]. Currey et al. have shown that water affects the viscoelastic behavior of bone [43]. Dry bone exhibits lower anelastic deformation as compared to wet bone. These indicate that water has significant influence on overall mechanical response of bone. However, the role of water on the nanostructure of bone, where the collagen is interacting with hydroxyapatite (HAP) nanocrystals, is not well understood. Here, we attempt to understand the mechanical response of wet collagen (solvated collagen) and compare it with dry collagen (unsolvated collagen) when interacting with HAP surface. This has been done using SMD simulations.

Table 1 Bone Composition (adapted from reference 19)

Components	Weight percentage
Hydroxyapatite	60
Collagen	20
Water	9
Ions and Non-collagenous proteins	11

In order to perform simulations, nano and molecular structure of collagen-HAP system should be understood clearly. At the nanoscale, bone consists of HAP mineralized at specific locations on collagen molecules [7]. Between the collagen molecules, HAP mineralizes in specific zones called as 'hole zones' (Figs. 1 and 2) [44, 45]. The mineralized HAP in these zones is hexagonal in structure with its *c*-axis aligned parallel to collagen fibers [46]. Collagen exhibits helical structure whereas its ends are non-helical and are known as N- or C-telopeptides [47–49]. Thus, collagen interacts with HAP through these telopeptides as shown in Fig. 2. We have constructed the model in a similar way as shown in Fig. 2. The main focus of the present modeling study with SMD simulations is to evaluate the role of mineral (HAP) and water on the load-deformation behavior of collagen molecule in close proximity of HAP.

Simulation Details

NAMD [50] has been used to perform MD and SMD simulations using CHARMm (Chemistry at Harvard Macromolecular mechanics) force field [51] and VMD [52] has been used for all the interactive studies and visualization.

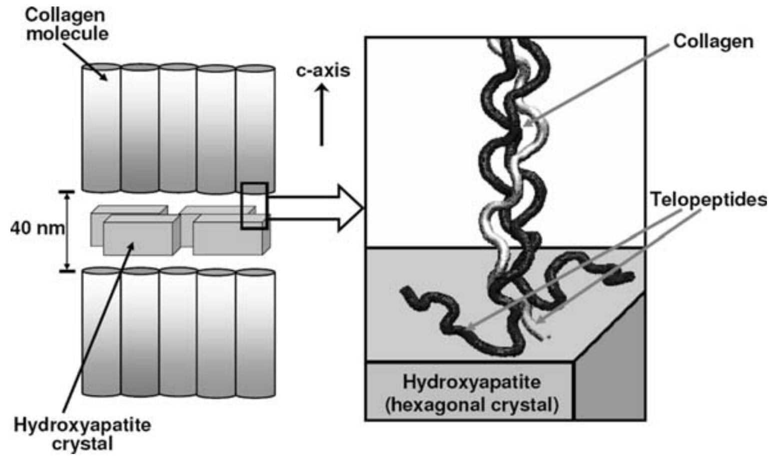

Fig. 2 The HAP-Collagen Interface

NAMD has been developed by theoretical and computational biophysics group at the Beckham Institute for Advanced Science and Technology at the University of Illinois at Urbana-Champaign. Minimization has been performed by conjugate gradient method on all models before performing MD and SMD simulations. Isothermal and isobaric ensemble (NPT) is used for MD and SMD simulations with periodic boundary conditions. Electrostatic interactions between pairs are calculated by Particle Mesh Ewald (PME) technique. The van der Waals cut off distance of 9 Å has been used in all simulations. Temperature of all models is controlled by Langevin dynamics and pressure is increased to 1.01 bar in steps and is calculated by Nose-Hoover Langevin piston method [53, 54]. Verlet algorithm is used to integrate the Newton equation of motion [53, 54]. MD simulations have been performed on all models followed by SMD simulations.

Model Construction And Simulations

Collagen Molecule with N-Telopeptide

The collagen is a triple helix molecule with three polypeptide chains with each polypeptide chain forming a left-handed helix that is folded in a right-handed superhelix [55]. The structure of collagen molecule with telopeptide is obtained from literature [49], where the $(GPP)_n$ model of collagen was obtained from the Protein Data Bank-ID 1 k6f.pdb [56]. Further, N-terminal telopeptide sequence used in the simulations is as follows [57, 58]:

α1-GlnLeuSerTyrGlyTyrAspGluLysSerThrGlyIleSerValPro-helix (GlyProMet-)
α2-GlnPheAspAlaLysGlyGlyGlyPro-helix (GlyProMet-)
The three stranded N-telopeptide are joined to triple helix molecule (GPP).

First, collagen molecule with N-terminal telopeptide (N-Collagen) is geometrically optimized through energy minimization using CHARMm force field [51]. Further, the optimized model is solvated with 1800 TIP3P water molecules followed by energy minimization of the solvated N-Collagen. Furthermore, the temperature is increased to 300 K from 0 K in steps of 100 K followed by increasing pressure from 0 bar to 1.01 bar in steps of 0.25 bar. The resulting structure has been used to perform SMD simulations in absence of HAP. The same geometrically optimized N-Collagen molecule has been used with HAP for interaction studies. In order to analyze the role of water on the overall mechanical response of N-Collagen, unsolvated N-Collagen is also used for SMD simulations in close proximity and in absence of HAP. Here, again the same route has been taken to obtain unsolvated N-Collagen molecule for SMD simulations.

HAP crystal model

HAP mineral has a hexagonal structure with space group $P6_3/m$ [59]. The unit cell parameters are $a = 9.424$ Å, $b = 9.424$ Å, $c = 6.879$ Å, $\alpha = 90°$, $\beta = 90°$, $\gamma = 120°$. The dimensions of the HAP used in the present study are $a = 75.392$ Å, $b = 75.392$ Å, $c = 20.637$ Å, $\alpha = 90°$, $\beta = 90°$, $\gamma = 120°$ which correspond to 192 unit cells of HAP i.e., 8 unit cells along *a*-axis, 8 unit cells along *b*-axis and 3 unit cells along *c*-axis. The dimensions of periodic boundary conditions are the same as dimensions of the HAP model used. CHARMm force field parameters for HAP have been obtained from our previous study of interfaces between HAP and polyacrylic acid [60, 61]. The constructed HAP model is first geometrically optimized through energy minimization then its temperature is increased from 0 K to 300 K in steps of 100 K. Further, pressure is increased to 1.01 bar in steps of 0.25 bar. Finally, the model is again geometrically optimized through energy minimization. The optimized model has been used to create appropriate surfaces. It has been found from experiments that the *c*-axis of HAP aligns parallel to collagen molecule, i.e. (0001) surface of HAP interacts with telopeptide of collagen molecule (Fig. 2). The (0001) surface of HAP has been created by extending the *c*-axis of HAP model from 20.637 Å to 320.637 Å which creates 300 Å of vacuum between (0001) surface of HAP and its periodic image. This creates a pseudo 2D periodic boundary condition from 3D periodic boundary condition. The (0001) surface of HAP is rendered non-dipolar by removing half of the surface ions (calcium atoms) from (0001) surface to its opposite surface. The construction of non-dipolar surface from dipolar surface has been performed in accordance with Tasker et al. [62]. The non-dipolar surface has been constructed because it has been observed previously that these surfaces are stable as compared to dipolar surfaces [63]. The HAP model with (0001) surface is geometrically optimized through energy minimization and then the temperature is increased from 0 K to 300 K in steps of 100 K. Further, pressure is increased to 1.01 bar. Finally, the model is geometrically optimized in order to obtain the structure of the model at the global energy minimum. This optimized model has been used with solvated and unsolvated N-Collagen to construct HAP-Collagen model.

Hydroxyapatite with N-Collagen molecule (HAP-Collagen)

The optimized model of solvated and unsolvated N-Collagen is brought in close proximity of minimized model of HAP with (0001) surface separately (HAP-Collagen) (Fig. 3). The model thus constructed is first geometrically optimized through energy minimization. Further, the same procedure is used to reach a temperature of 300 K at a pressure of 1.01 bar as mentioned in the previous sections. Finally, such created HAP-Collagen model is used for SMD simulations.

Steered molecular dynamics (SMD) simulations

SMD simulation is a type of MD simulation technique in which force is applied to selected atom/atoms. It provides the dynamics of binding and unbinding of analyzed molecules with applied load [64–74]. It also provides the mechanical response of molecules. SMD simulations can be conducted at: constant force [64, 75] and constant velocity [64–67, 76]. We have used constant velocity SMD (v-SMD) in which constant velocity is applied to selected atom/atoms. Force is calculated in v-SMD as $F = k(vt–x)$, where k is the spring constant of the spring attached to the pulled atom/atoms, and v is the pulling velocity, t is the time and x is displacement. In order to analyze the response of N-Collagen molecule under load, the center of mass of N-Collagen has been pulled at a velocity of 1 Å/ps. The force constant of the spring is 4.0 kcal mol^{-1}Å^{-2} which corresponds to spatial (thermal) fluctuation of the center of mass of 0.77 Å $\left(\sqrt{k_B T/k}\right)$ [77] at 300 K. The ends of the telopeptides chains are fixed (carbonyl carbon atoms of pyroglutamic acid residues of all the chains). In order to analyze the load-deformation behavior of N-Collagen, the center of mass of the N-Collagen is pulled in close proximity of HAP and in absence of HAP. To understand the role of water on the load-deformation behavior, another type of v-SMD simulations have been performed in which center of mass of solvated and unsolvated N-Collagen is pulled in close proximity of HAP separately and the layers of HAP opposite to (0001) surface are fixed (Fig. 4).

Interaction energy calculation

The interaction energy between the components has been evaluated by energy evaluation tool of NAMD, MDEnergy^{TM} [50]. Here, energy is calculated between defined atoms using a specified cut-off distance. This

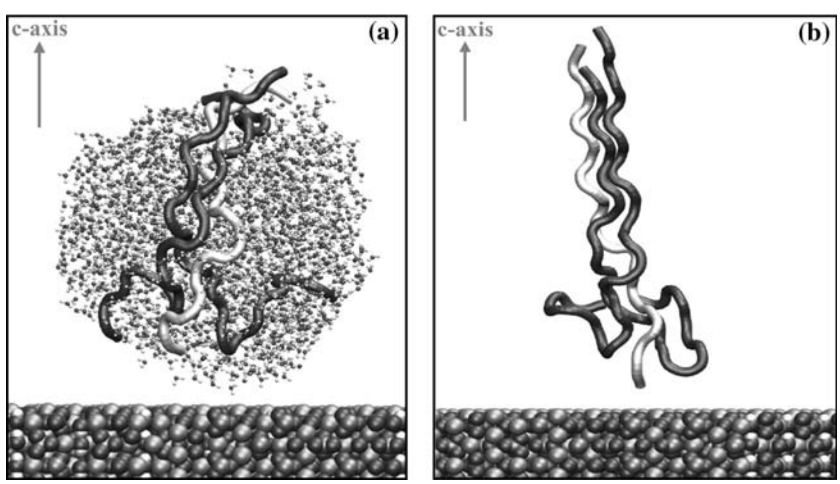

Fig. 3 Minimized models of (**a**) Solvated and (**b**) Unsolvated N-Collagen interacting HAP surface (N-Collagen molecules are represented in Tube (α1 chains are in black color whereas α2 chain is in white color), Water is represented by ball and stick representations, and HAP is represented in VDW)

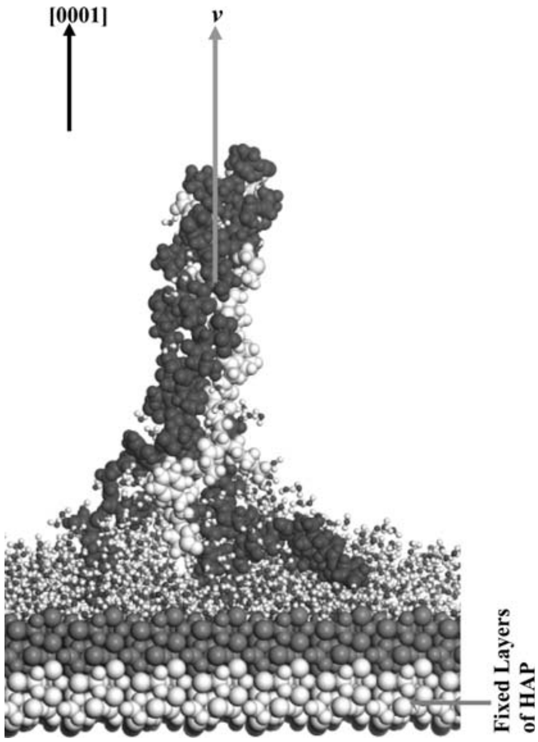

Fig. 4 Pulling of solvated N-Collagen in close proximity of HAP. Here Layers opposite to (0001) surface of HAP were fixed (as shown in white color) (N-Collagen molecules are represented in VDW (α1 chains are in black color whereas α2 chain is in white color), Water is represented in ball and stick, and HAP is represented in VDW)

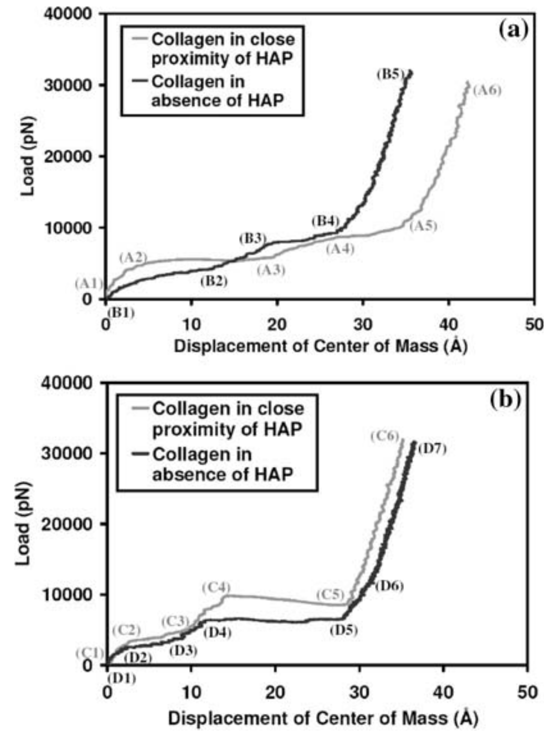

Fig. 5 Load-Deformation plots of (**a**) Solvated and (**b**) Unsolvated collagen molecule in close proximity and in absence of HAP

technique uses the trajectory file obtained during simulations, the topology file of the structure, and the parameter file. The interaction energy between the atoms has been calculated for the entire 150 ps of v-SMD simulations.

Results and discussion

Figure 5a shows the load-deformation response of solvated N-Collagen in close proximity (grey) and in absence (black) of HAP (Fig. 6). The load-deformation behavior of N-Collagen in close proximity of HAP shows five distinct regions and they are represented as A1A2, A2A3, A3A4, A4A5, and A5A6. The slopes of these regions represent the stiffness of N-Collagen when HAP is present. The change in slope corresponds to unbinding and binding events occurring at different time intervals. The region A1A2 results from the interaction of N-Collagen with water molecules and with HAP molecule. The change in slope from region A1A2 to A2A3 results from unbinding of N-Collagen from water molecules that are interacting with N-Collagen and HAP surface. The regions A3A4 and A4A5 result from breaking of hydrogen bonds between proline and glycine residues of helical regions of N-Collagen, and also from unbinding of water molecules from N-Collagen. Finally, the region A5A6 is attributed to the backbone chain of the N-Collagen molecule. Similarly, the same type of behavior is also obtained for N-Collagen in absence of HAP as shown in Fig. 5a. However, the region A2A3 which has been obtained for the N-Collagen in presence of HAP is not observed for the N-Collagen in absence of HAP. The reason for this is that at the start of the region A2A3 (in the plot for N-Collagen in presence of HAP), N-Collagen unbinds from the water molecules and the water molecules interact with the charged surface of HAP, whereas in the absence of HAP, there is absence of interaction of water molecules with any surface.

In order to understand the role of water on the mechanics of N-Collagen, unsolvated N-Collagen is also used and is shown in Fig. 5b, where pulling of unsolvated N-Collagen in close proximity of HAP is represented by grey color whereas the pulling of unsolvated N-Collagen in absence of HAP is represented by black color. The response of N-Collagen in close proximity of HAP exhibits five regions: C1C2, C2C3, C3C4, C4C5, and C5C6 whereas the N-Collagen in absence of HAP exhibits six regions: D1D2, D2D3, D3D4, D4D5, D5D6, and D6D7. A similar type of trend has been observed for several proteins when pulled at constant velocity [71, 78]. The regions C5C6 and D6D7 result from backbone chain of N-Collagen. On comparing the slopes of regions A1A2

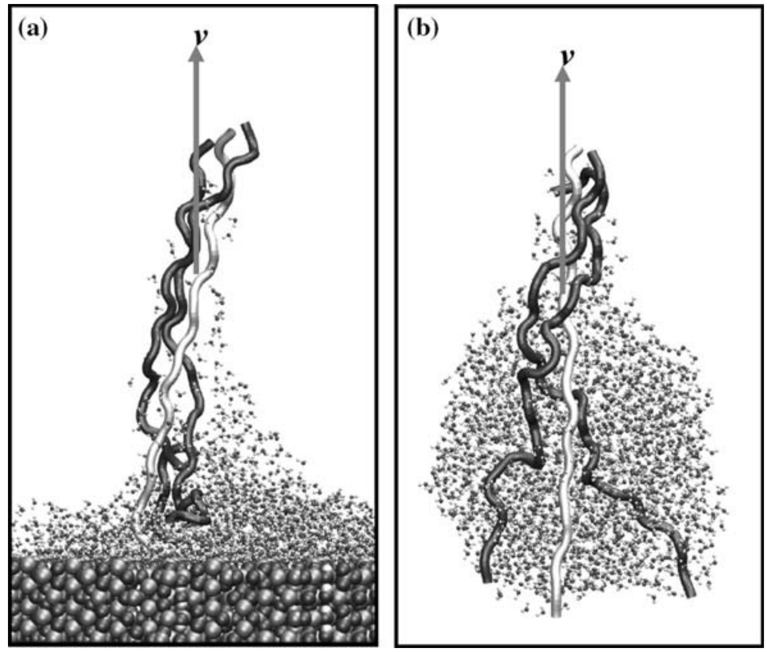

Fig. 6 Pulling of Solvated N-Collagen (**a**) in close proximity of HAP and (**b**) in absence of HAP (Here telopeptide ends are fixed)

(44.93 kcal mol^{-1}Å^{-2}) and B1B2 (53.03 kcal mol^{-1}Å^{-2}), of solvated N-Collagen with the slopes of the regions C1C2 (53.24 kcal mol^{-1}Å^{-2}) and D1D2 (57.92 kcal mol^{-1}Å^{-2}) of unsolvated N-Collagen, it has been observed that the slopes of these regions are similar. This indicates that the presence of HAP and water does not affect stiffness of the backbone chain of N-Collagen molecule. However, the peak loads of solvated and unsolvated N-Collagen molecules in close proximity of HAP are 10600 pN and 9700 pN respectively, at displacements of 34.7 Å and 15.6 Å respectively. These are observed as peak loads when the contribution of the backbone of N-Collagen is not significant in the load-deformation response. Similarly, we have observed that the peak loads of solvated and unsolvated N-Collagen molecules in absence of water are 10000 pN and 6500 pN with displacements 27.7 Å and 15.6 Å respectively. This indicates that water influences the load-deformation response of N-Collagen. In order to analyze the role of water on the interaction of N-Collagen with HAP, another type of v-SMD simulations have been performed as mentioned in the SMD section. Here, solvated and unsolvated N-Collagen molecules are pulled in close proximity of HAP while keeping the layers opposite to (0001) surface of HAP fixed (Fig. 7). The load-deformation response thus obtained is shown in Fig. 8a, b. The area under the load-deformation plot represents the energy needed by a molecule to deform. The area under the plots of Fig. 8a, b represents the energy needed by solvated and unsolvated molecule to untie from the HAP surface. On comparing the area of the load-deformation response of solvated and unsolvated N-Collagen in close proximity of HAP, it has been observed that the solvated N-Collagen requires more energy (296.87 kcal/mol) to untie from the surface as compared to the unsolvated N-Collagen molecule (210.34 kcal/mol). This comparison has been performed for displacement of center of mass up to 50 Å as beyond 50 Å, the area does not change significantly. To understand the attachment of N-Collagen molecule with HAP, interaction energy between various components during v-SMD simulations has been calculated using MDEnergy$^{\mathrm{TM}}$ as shown in Fig. 9. During v-SMD simulations, interaction energy between HAP-water is highest followed by interaction energy between collagen-water and then between HAP-collagen. Although significant changes are apparent in the load-deformation response as shown in Fig. 7, the corresponding changes are not significant in the Energy-Time plot (Fig. 9). This indicates that the interaction between HAP and N-Collagen occurs through water i.e., the load is transferred to HAP from N-Collagen through the water molecules present between HAP and N-Collagen.

Conclusions

Bone exhibits a complex structural hierarchy that spans over nanometer to millimeter. At the nanostructural level, bone is primarily composed of HAP and collagen. Here, we have evaluated the load-deformation behavior of N-Collagen molecules in close proximity and in absence of HAP using v-SMD simulations. It has been observed that the load-deformation response of solvated N-collagen in close proximity of HAP has features which result from breaking

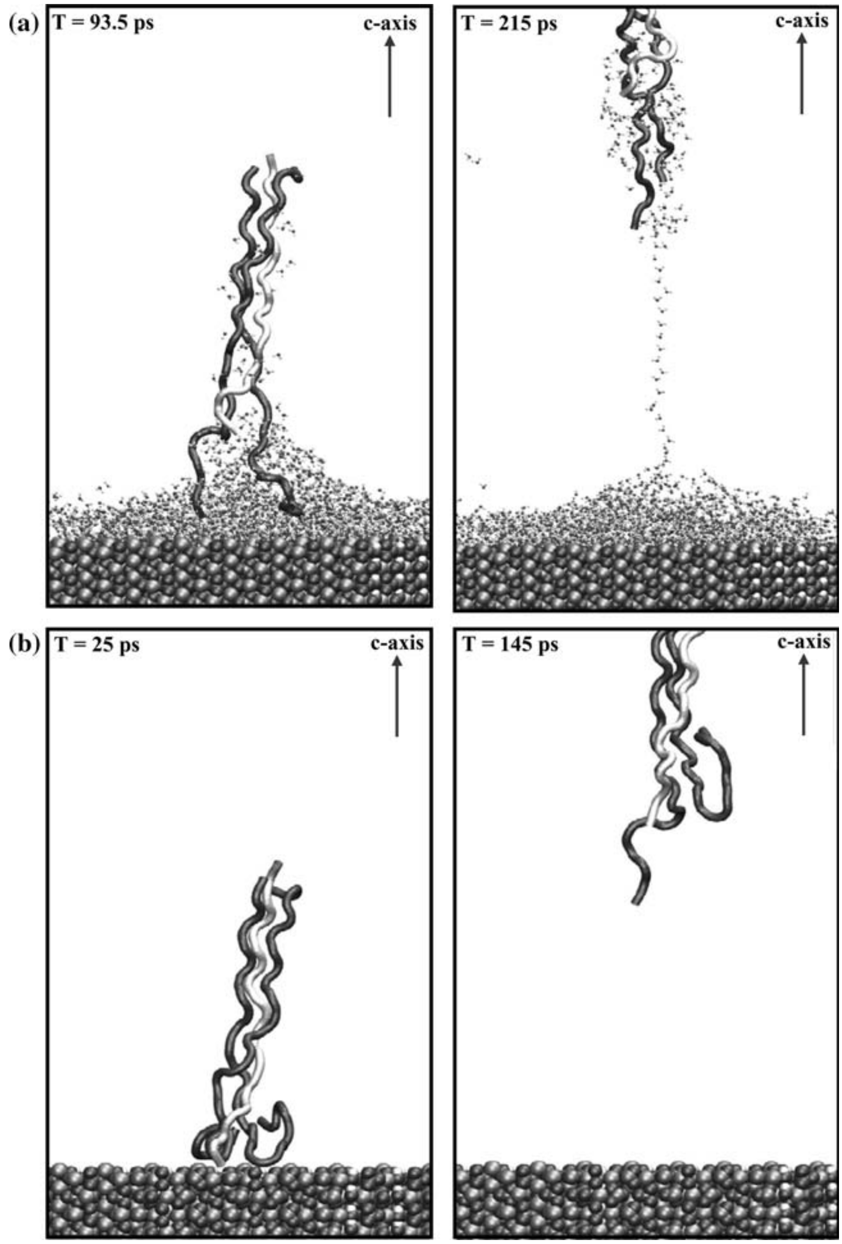

Fig. 7 Pulling of (**a**) Solvated and (**b**) Unsolvated N-Collagen in close proximity of HAP along c-axis (along [0001] direction) during different time (Here layers opposite to (0001) surface are fixed)

of hydrogen bonds between N-Collagen and water, where water is interacting with HAP significantly. These features are not present in the plot for N-Collagen in absence of HAP due to lack of interaction between water and HAP. The load-deformation response for solvated N-Collagen differs from the load-deformation response of unsolvated N-Collagen. To understand the role of water on the load-deformation response of N-Collagen in close proximity of HAP, solvated and unsolvated N-Collagen molecules are pulled separately in close proximity of HAP. It has been observed from the plots of load-deformation response that the solvated N-Collagen requires more energy to untie from the HAP surface as compared to unsolvated N-Collagen. We have shown from the energy-time plots of various pairs that N-Collagen interacts with HAP through water.

The present study is focused on the influence of mineral and water on the load deformation behavior of N-Collagen in HAP-Collagen model system. This model system is the initial step towards understanding the molecular and nano mechanical response of bone. However, in order to predict the molecular and nano mechanical response of bone accurately, the present model needs to incorporate several complex molecular and nano features of bone such as intergrowth. Also, in order to evaluate the mechanical response of nano and molecular structure of real bone

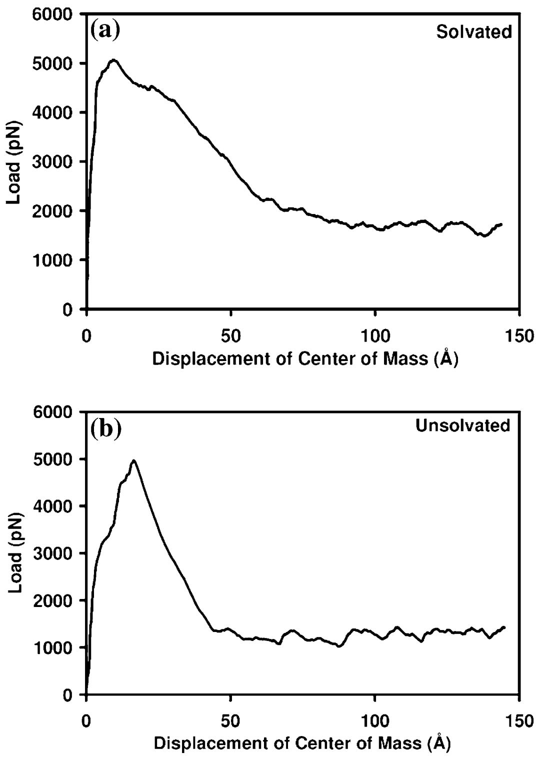

Fig. 8 Load-deformation plots of (**a**) solvated and (**b**) unsolvated collagen in close proximity of HAP (Here layers opposite to (0001) surface are fixed)

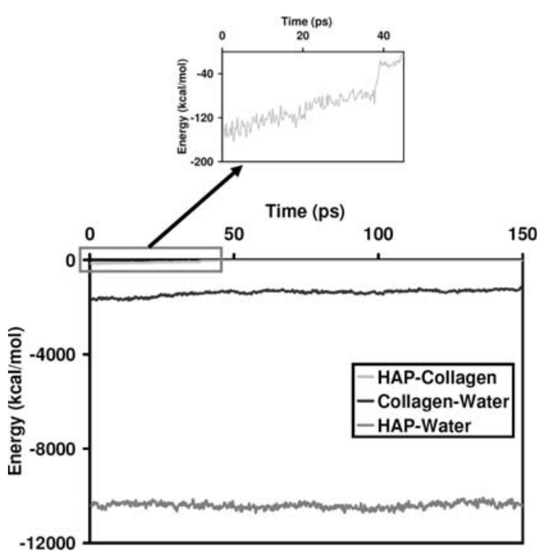

Fig. 9 Total interaction energy between HAP-collagen, collagen-water and HAP-water

accurately, the present model would require more parameters to include the complex nano and molecular structural features of real bone. However, the present study is a first step in the process and has shown that mineral and water influence the load-deformation behavior of N-Collagen.

Acknowledgments This research is partially funded by grant from National Science Foundation (CAREER grant # 0132768). The computational resources provided by National Center of Superconducting applications (NCSA) at University of Illinois at Urbana-Champaign (UIUC) through Teragrid are acknowledged. The authors would also like to acknowledge Dr. Gregory H. Wettstein and Francis Larson of Center for High Performance Computing (CHPC), NDSU.

References

1. Marieb EN (1998) In: Human anatomy & physiology, 4th edn. Benjamin/Cummings Science Publishing, Menlo Park, California
2. Tortora GJ (1989) In: Principles of human anatomy, 5th edn. Harper & Row Publishers, New York
3. Boyle WJ, Simonet WS, Lacey DL (2003) Nature 423:337
4. Von Recum AF (1998) In: Handbook of biomaterials evaluation. CRC Publisher
5. Ramakrishna S, Mayer J, Wintermantel E, Leong WK (2001) Comp Sci Tech 61:1189
6. Black J (1992) In: Biological performance of materials: fundamentals of biocompatibility. Marcel Dekker, New York
7. Weiner S, Wagner HD (1998) Ann Rev Mater Res 28:271
8. Weiner S, Traub W (1992) FASEB 6:879
9. Landis WJ (1995) Bone 16:533
10. Katti KS, Gujjula P (2002) In: Proceedings of 15th ASCE engineering mechanics conference, New York, NY
11. Verma D, Katti K, Katti D (2006) J Biomed Mater Res 77:59
12. Verma D, Katti K, Katti D (2006) J Biomed Mater Res 78A:772
13. Katti KS, Turlapati P, Verma D, Bhowmik R, Gujjula P, Katti DR (2006) Am J Biochem Biotech 2:73
14. Katti KS (2004) Colloids Interfaces B 39:133
15. Gao H, Ji B, Jäger IL, Arzt E, Fratzl P (2003) Proc Natl Acad Sci USA 100:5597
16. Gao H, Chen S (2005) J Appl Mech 72:732
17. Ji B, Gao H (2004) Mater Sci Eng A 366:96
18. Ji B, Gao H (2004) J Mech Phys Solids 52:1963
19. Ji B, Gao H, Hsia KJ (2004) Phil Mag Lett 84:631
20. Gao H, Ji B (2003) Eng Frac Mech 70:1777
21. Ji B, Gao H (2006) Comp Sci & Tech 66:1212
22. Buehler MJ (2006) PNAS 103:12285
23. Buehler MJ (2006) J Mat Sci 21:1947
24. Hellmich C, Barthélémy J-F, Dormieux L (2004) Eur J Mech A/Solids 23:783
25. Fritsch A, Hellmich C (2007) J Theor Biol 244:597
26. Reilly DT, Burstein AH, Frankel VH (1974) J Biomech 7:271
27. Rho JY, Tsui TY, Pharr GM (1997) Biomaterials 18:1325
28. Murugan R, Ramakrishna S (2005) Comp Sci & Tech 65:2385
29. Jae-Young Rho L. Kuhn-Spearing, Zioupos P (1998) Med Eng & Phy 20:92
30. Landis WJ (1995) Bone 16:533
31. Ziv V, Weiner S (1994) Conn Tissue Res 30:165
32. Ghosh P, Katti DR, Katti KS (2007) Biomacromolecules 8:851
33. Legeros RZ (1994) In: Biological and synthetic apatites. CRC Press, Boca Raton
34. Park JB (1984) In: Biomaterials science and engineering. Plenum Press, New York
35. Murugan R, Ramakrishna S (2004) In: Encyclopedia of nanoscience and nanotechnology, vol 7. American Scientific Publishers, California, p 595
36. Dempster WT, Liddicoat RT (1952) Am J Anatomy 91:331
37. Evans FG (1973) Mechanical properties of bone. Thomas, Springfield
38. Evans FG, Lebow M (1951) J Appl Physiol 3:563

39. Sedlin ED, Hirsch C (1966) Acta Orthopaedica Scandinavica 37:29
40. Smith JW, Walmsley R (1959) J Anatomy 93:503
41. Yamada H, Evans FG (1970) Strength of biological materials. Williams & Wilkins, Baltimore
42. Nyman JS, Roy A, Shen X, Acuna RL, Tyler JH Wang X (2006) J Biomech 39:931
43. Currey JD (1965) J Exp Biol 43:279
44. Fitton-Jackson S (1957) Proc R Soc London Ser B 146:270
45. Nylen MU, Scott DB, Mosley VM (1960) In: Sognnaes RF (ed) Calcification in Biological Systems. Am Assoc Adv Sci p 129
46. Itoha S, Masanori K, Koyamac Y, Takakudac K, Shinomiyaa K, Tanaka J (2002) Biomaterials 23:3919
47. Kadler KE, Holmes DF, Trotter JA, Chapman JA (1996) Biochem J 316:1
48. Malone JP, Alvares K, Veis A (2005) Biochem 44:15269
49. Malone JP, George A, Veis A (2004) Proteins: Struct Funct & Biol 54:206
50. Kale L, Skeel R, Bhandarkar M, Brunner R, Gursoy A, Krawetz N, Phillips J, Shinozaki A, Varadarajan K, Schulten KJ (1999) Comput Phys 151:283 http://www.ks.uiuc.edu/Research/namd/, as on 16 January 2007
51. Brooks BR, Bruccoleri RE, Olafson BD, States DJ, Swaminathan S, Karplus MJ (1983) J Comput Chem 4:187
52. Humphrey W, Dalke A, Schulten KJ (1996) J Mol Graphics 14:33, http://www.ks.uiuc.edu/Research/vmd/, as on 16 January 2007
53. Feller SE, Zhang Y, Pastor RW, Brooks BR (1995) J Chem Phys 103:4613
54. Martyna GJ, Tobias DJ, Klein ML (1994) J Chem Phys 101:4177
55. Beck K, Brodsky B (1998) J Struct Biol 122:17
56. Berisio R, Vitagliano L, Mazzarella L, Zagari A (2002) Protein Sci 11:262
57. Jones EY, Miller A (1987) Biopolymers 26:463
58. Otter A, Kotovych G, Scott PG (1989) Biochemistry 28:8003
59. Sudarsanan K, Young RA (1969) Acta Crystallographica B 25:1534
60. Bhowmik R, Katti KS, Verma D, Katti DR (2007) Mater Sci Eng C 27:352
61. Bhowmik R, Katti KS, Katti D (2006) Polymer 48:664
62. Tasker PW (1979) J Phys C Solid State Phys 12:4977
63. Bertaut FCR (1958) Acad Sci Paris 246:3447
64. Izrailev S, Stepaniants S, Balsera M, Oono Y, Schulten K (1997) Biophys J 72:1568
65. Isralewitz B, Izrailev S, Schulten K (1997) Biophys J 73:2972
66. Wriggers W, Schulten K (1999) Proteins Struct Funct Genet 35:262
67. Kosztin D, Izrailev S, Schulten K (1999) Biophys J 76:188
68. Molnar F, Ben-Nun M, MartíNez TJ, Schulten K (2000) J Mol Struct (THEOCHEM) 506:169
69. Lu H, Isralewitz B, Krammer A, Vogel V, Schulten K (1998) Biophys J 75:662
70. Krammer A, Lu H, Isralewitz B, Schulten K, Vogel V (1999) Proc Natl Acad Sci USA 96:1351
71. Lu H, Schulten K (1999) Proteins Struct Funct Genet 35:453
72. Lu H, Schulten K (1999) Chem Phys 247:141
73. Izrailev S, Stepaniants S, Isralewitz B, Kosztin D, Lu H, Molnar F, Wriggers W, Schulten K (1998) In: Computational molecular dynamics: challenges, methods, ideas. volume 4 of Lecture Notes in Computational Science and Engineering, Springer-Verlag, Berlin p 39
74. Schulten K, Schulten Z, Szabo A (1981) J Chem Phys 74:4426
75. Lu H, Krammer A, Isralewitz B, Vogel V, Schulten K (2000) In: Elastic filaments of the cell. Academic/Plenum Publishers, New York, p 143
76. Grubmüller H, Heymann B, Tavan P (1996) Science 271:997
77. Balsera M, Stepaniants S, Oono Y, Schulten K (1997) Biophys J 73:1281
78. Gao M, Wilmanns M, Schulten K (2002) Biophysical J 83:3435